A Hydrogen Load Modeling Method for Integrated Hydrogen Energy System Planning

Preprint

Xinyi Zhao,[1,2] Yiyun Yao,[1] Weijia Liu,[1] Rishabh Jain,[1] and Chaoyue Zhao[2]

1 National Renewable Energy Laboratory
2 University of Washington

Presented at the 2023 IEEE Conference on Innovative Smart Grid Technologies North America (ISGT NA)
Washington, D.C.
January 16–19, 2023

NREL is a national laboratory of the U.S. Department of Energy
Office of Energy Efficiency & Renewable Energy
Operated by the Alliance for Sustainable Energy, LLC

This report is available at no cost from the National Renewable Energy Laboratory (NREL) at www.nrel.gov/publications.

Contract No. DE-AC36-08GO28308

Conference Paper
NREL/CP-5D00-83894
January 2023

A Hydrogen Load Modeling Method for Integrated Hydrogen Energy System Planning

Preprint

Xinyi Zhao,[1,2] Yiyun Yao,[1] Weijia Liu,[1] Rishabh Jain,[1] and Chaoyue Zhao[2]

1 National Renewable Energy Laboratory
2 University of Washington

Suggested Citation
Zhao, Xinyi, Yiyun Yao, Weijia Liu, Rishabh Jain, and Chaoyue Zhao. 2023. *A Hydrogen Load Modeling Method for Integrated Hydrogen Energy System Planning: Preprint*. Golden, CO: National Renewable Energy Laboratory. NREL/CP-5D00-83894. https://www.nrel.gov/docs/fy23osti/83894.pdf.

NREL is a national laboratory of the U.S. Department of Energy
Office of Energy Efficiency & Renewable Energy
Operated by the Alliance for Sustainable Energy, LLC

This report is available at no cost from the National Renewable Energy Laboratory (NREL) at www.nrel.gov/publications.

Contract No. DE-AC36-08GO28308

Conference Paper
NREL/CP-5D00-83894
January 2023

National Renewable Energy Laboratory
15013 Denver West Parkway
Golden, CO 80401
303-275-3000 • www.nrel.gov

NOTICE

This work was authored in part by the National Renewable Energy Laboratory, operated by Alliance for Sustainable Energy, LLC, for the U.S. Department of Energy (DOE) under Contract No. DE-AC36-08GO28308. Funding provided by U.S. Department of Energy Office of Energy Efficiency and Renewable Energy Hydrogen and Fuel Cell Technologies Office under agreement 38784. The views expressed herein do not necessarily represent the views of the DOE or the U.S. Government.

Cover Photos by Dennis Schroeder: (clockwise, left to right) NREL 51934, NREL 45897, NREL 42160, NREL 45891, NREL 48097, NREL 46526.

A Hydrogen Load Modeling Method for Integrated Hydrogen Energy System Planning

Xinyi Zhao[1,2], Yiyun Yao[1], Weijia Liu[1], Rishabh Jain[1], Chaoyue Zhao[2]

[1]National Renewable Energy Laboratory
Golden, CO, U.S.A.
{xinyi.zhao; yiyun.yao; weijia.liu; rishabh.jain}@nrel.gov

[2]University of Washington
Seattle, WA, U.S.A.
cyzhao@uw.edu

***Abstract* — The integrated hydrogen energy system incorporates hydrogen energy into the power grid, which has been recognized as a promising option for reaching a 100% renewable electricity supply. It can make a profit because the hydrogen produced can be sold as fuel or used to generate electricity for grid services. In this paper, we develop a planning model for the integrated hydrogen energy system that considers the uncertainty of the load demand, the renewable energy generation, and the market prices. To calculate the hydrogen load, we simulate the refueling operations at a hydrogen fueling station over the course of one day and generate representative load profiles with K-means clustering. Moreover, the long-term profitability of the integrated system under both current and future conditions is validated in 10-year planning results.**

***Index Terms* – Integrated hydrogen energy system, renewable electricity, grid service, hydrogen load simulation, profitability**

I. Introduction

To become energy sufficient and reduce carbon emissions, we need to increase the penetration of renewable energy sources in the current power system. Renewable generation, such as solar power, can be intermittent and need to be curtailed when the load demand is insufficient [1]. Because of the high energy density of approximately 120 MJ/kg [2], hydrogen appears promising for storing excess renewable electricity and using it during peak load periods. However, the production and storage of hydrogen are prohibitively expensive, which, at present, block its path to becoming the lowest-cost option.

A substantial body of research has been reported on the long-term profitability of hydrogen energy systems for industrial [3] and residential applications [4]. Schrotenboer et al. [5] investigate the integration of hydrogen storage systems with wind power plants and demonstrate how hydrogen storage can increase the operational revenue from the electricity and hydrogen markets. Jingqi et al. [6] propose the siting and sizing model for hydrogen refueling stations while demonstrating that the profitability of these stations will increase in the future due to lower costs. Most research, however, focuses on hydrogen storage used for peak load shifting, with other ancillary services, such as frequency regulation, being overlooked [7]. Further, few studies present a simulation model of the hydrogen fueling load. Hence, we develop a planning model of integrated systems that incorporates the hydrogen energy system into the power grid with Photovoltaic (PV) generation and Electric Vehicle (EV) load. Based on the number of arriving trucks and their fueling time, the load demand of hydrogen-fueled trucks is simulated. With consideration of providing multiple grid services and selling hydrogen as fuel, the profitability of the integrated system in 10 years is tested. The rest of this paper is organized as follows. Section II details the objective and constraints for the planning model. Section III presents a simulation model of the hydrogen-fueled trucks in a fueling station. Section IV demonstrates the profitability of the planning model in three cases. Section V contains the conclusion.

II. Integrated System Planning Model

In this section, we develop a planning model for an integrated hydrogen energy system (shown in Fig. 1) that can be coupled with both electricity and hydrogen. In addition to the hydrogen energy system, we incorporate the PV and EVs into the planning model.

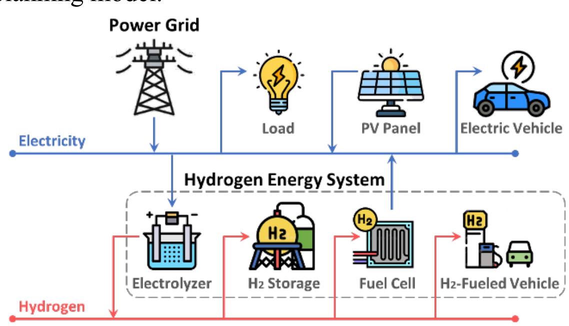

Fig. 1 System diagram of an integrated hydrogen energy system.

A. Objective Function

The overall planning cost in the integrated system is presented with four terms, as shown in (1):

$$\min \;\; C_{\text{total}} = C_{\text{inv}} + \textstyle\sum_s \theta_s (C_{\text{op}}^s - C_{\text{re,e}}^s - C_{\text{re,h}}^s + C_{\text{pe,e}}^s) \quad (1)$$

where C_{total} and C_{inv} denote the annual planning cost and investment cost, respectively. C_{op}^s is the system operating cost in scenario s. $C_{\text{re,e}}^s$ and $C_{\text{re,h}}^s$ are the revenue to provide grid services and satisfy the hydrogen load in scenario s, respectively.

This work was authored in part by the National Renewable Energy Laboratory, operated by Alliance for Sustainable Energy, LLC, for the U.S. Department of Energy (DOE) under Contract No. DE-AC36-08GO28308. Funding provided by the U.S. Department of Energy Office of Energy Efficiency and Renewable Energy Hydrogen and Fuel Cell Technologies Office under agreement 38784. The views expressed in the article do not necessarily represent the views of the DOE or the U.S. Government.

$C_{\mathrm{pe,e}}^{s}$ represents the penalty for failing to provide the requested grid services, and θ_s is the weight of the scenario s.

We assume that in the planning scheme, all investment decisions are made at the beginning of the planning period. In (2), the cost C_{inv} is expressed as the annuity of a one-time investment based on the planning year n and the interest rate α:

$$C_{\mathrm{inv}} = \frac{\alpha(1+\alpha)^{n-1}}{(1+\alpha)^{n}-1}\left(C_{\mathrm{HS,inv}} + C_{\mathrm{PV,inv}} + C_{\mathrm{EV,inv}}\right) \quad (2)$$

where $C_{\mathrm{HS,inv}}$, $C_{\mathrm{PV,inv}}$, and $C_{\mathrm{EV,inv}}$ denote the investment payments of the integrated system, PV, and EVs. $C_{\mathrm{HS,inv}}$ can be further divided into four parts [6]:

$$C_{\mathrm{HS,inv}} = c_{\mathrm{tank}} \cdot S_{\mathrm{tank}} + c_{\mathrm{EL}} \cdot S_{\mathrm{EL}} + c_{\mathrm{FC}} \cdot S_{\mathrm{FC}} + c_{\mathrm{fixed}} \quad (3)$$

where c_{tank}, c_{EL}, and c_{FC} denote the unit investment costs of the hydrogen storage tank, electrolyzers, and fuel cells. Correspondingly, S_{tank}, S_{EL}, and S_{FC} denote the size of the hydrogen storage tank, electrolyzers, and fuel cells, respectively. c_{fixed} is the fixed investment cost for a hydrogen energy system.

The annual operating cost C_{op}^{s} includes the net energy procurement cost and the maintenance costs:

$$C_{\mathrm{op}}^{s} = \sum_t\left(\lambda_{\mathrm{TOU}}^{s,t} P_{\mathrm{im}}^{s,t} - \lambda_{\mathrm{mcp}}^{s,t} P_{\mathrm{ex}}^{s,t}\right) + C_{\mathrm{HS,op}} + C_{\mathrm{PV,op}} + C_{\mathrm{EV,op}} \quad (4)$$

where $\lambda_{\mathrm{TOU}}^{t}$ and $\lambda_{\mathrm{mcp}}^{t}$ denote the time-of-use (TOU) electricity price and the market clearing price, respectively. P_{im}^{t} and P_{ex}^{t} represent the imported and exported power of the integrated system at time t. $C_{\mathrm{HS,op}}$, $C_{\mathrm{PV,op}}$, and $C_{\mathrm{EV,op}}$ denote the maintenance costs of the hydrogen energy system, PV, and EVs.

The grid-side income $C_{\mathrm{re,e}}^{s}$ includes three parts: the revenue from demand response, the compensation to support the EV charging load, and the revenue from frequency regulation:

$$C_{\mathrm{re,e}}^{s} = \lambda_{\mathrm{DR}} P_{\mathrm{DR}} + \sum_t\left(\lambda_{\mathrm{EV}} P_{\mathrm{EV}}^{s,t} + \lambda_{\mathrm{RU}}^{s,t} P_{\mathrm{RU}}^{s,t} + \lambda_{\mathrm{RD}}^{s,t} P_{\mathrm{RD}}^{s,t}\right) \quad (5)$$

where λ_{DR}, λ_{EV}, $\lambda_{\mathrm{RU}}^{s,t}$, and $\lambda_{\mathrm{RD}}^{s,t}$ denote the energy compensation price, the EV compensation price, and the regulation-up and regulation-down service prices at time t. P_{DR}, $P_{\mathrm{EV}}^{s,t}$, $P_{\mathrm{RU}}^{s,t}$, and $P_{\mathrm{RD}}^{s,t}$ represent the demand response capacity, the EV load, and the regulation-up/down capacity of the integrated system.

Another revenue from selling hydrogen is illustrated in (6):

$$C_{\mathrm{re,h}}^{s} = \lambda_{\mathrm{H}} \sum_t F_{\mathrm{L,H}}^{s,t} \quad (6)$$

where λ_{H} denotes the hydrogen compensation price, and $F_{\mathrm{L,H}}^{s,t}$ denotes the hydrogen load demand at time t (unit: kg).

The final part of the total cost, as shown in (7), is the penalty for failing to provide the requested grid services:

$$C_{\mathrm{pe,e}}^{s} = \sum_t\left(\lambda_{\mathrm{DR,pe}} P_{\mathrm{DR,fail}}^{s,t} + \lambda_{\mathrm{RU,pe}}^{s,t} P_{\mathrm{RU,fail}}^{s,t} + \lambda_{\mathrm{RD,pe}}^{s,t} P_{\mathrm{RD,fail}}^{s,t}\right) \quad (7)$$

where $\lambda_{\mathrm{DR,pe}}$, $\lambda_{\mathrm{RU,pe}}^{s,t}$, and $\lambda_{\mathrm{RD,pe}}^{s,t}$ denote the penalty costs for the unsatisfied demand response, regulation-up/down services. $P_{\mathrm{DR,fail}}^{s,t}$, $P_{\mathrm{RU,fail}}^{s,t}$, and $P_{\mathrm{RD,fail}}^{s,t}$ represent the capacity of the unsatisfied demand response, regulation-up/down services at time t.

B. Constraints

To determine the optimal sizing of each component in the integrated hydrogen energy system, the planning model employs the four types of constraints listed below.

1) Power Balance:

To ensure the power balance within the integrated system shown in Fig. 1, we develop Eq. (8a)–(8c), where different grid services are requested at time t. Eq (8a) represents that no grid service is provided, whereas Eq. (8b) indicates that a required amount of load is curtailed as demand response, and Eq. (8c) represents that frequency regulation is provided. The net power import of the integrated system is also limited in (9) to denote the maximum capacity for peak load management:

$$P_{\mathrm{im}}^{s,t} - P_{\mathrm{ex}}^{s,t} = P_{\mathrm{HS,EL}}^{s,t} - P_{\mathrm{HS,FC}}^{s,t} + P_{\mathrm{EV}}^{s,t} + P_{\mathrm{L}}^{s,t} - P_{\mathrm{PV}}^{s,t} \quad (8a)$$

$$\begin{aligned} P_{\mathrm{im}}^{s,t} - P_{\mathrm{ex}}^{s,t} = {} & P_{\mathrm{HS,EL}}^{s,t} - P_{\mathrm{HS,FC}}^{s,t} + P_{\mathrm{EV}}^{s,t} + P_{\mathrm{L}}^{s,t} - P_{\mathrm{PV}}^{s,t} \\ & + \left(P_{\mathrm{DR}} - P_{\mathrm{DR,fail}}^{s,t}\right) \end{aligned} \quad (8b)$$

$$\begin{aligned} P_{\mathrm{im}}^{s,t} - P_{\mathrm{ex}}^{s,t} = {} & P_{\mathrm{HS,EL}}^{s,t} - P_{\mathrm{HS,FC}}^{s,t} + P_{\mathrm{EV}}^{s,t} + P_{\mathrm{L}}^{s,t} - P_{\mathrm{PV}}^{s,t} \\ & + \beta_{\mathrm{RU}}^{s,t}\left(P_{\mathrm{RU}}^{s,t} - P_{\mathrm{RU,fail}}^{s,t}\right) - \beta_{\mathrm{RD}}^{s,t}\left(P_{\mathrm{RD}}^{s,t} - P_{\mathrm{RD,fail}}^{s,t}\right) \end{aligned} \quad (8c)$$

$$P_{\mathrm{im}}^{s,t} - P_{\mathrm{ex}}^{s,t} \le \overline{P_{net}}, \forall s,t \quad (9)$$

where $P_{\mathrm{HS,EL}}^{s,t}$ and $P_{\mathrm{HS,FC}}^{s,t}$ denote the power input of the electrolyzers and the power output of the fuel cells in the hydrogen energy system. $P_{\mathrm{L}}^{s,t}$ is the predetermined load demand. $P_{\mathrm{PV}}^{s,t}$ represents the power output of the PV modules. $\beta_{\mathrm{RU}}^{s,t}$ and $\beta_{\mathrm{RD}}^{s,t}$ indicate whether to regulate up or down, with values of 1 or 0 (for example, $\beta_{\mathrm{RU}}^{s,t} = 1$ indicates that the regulation-up capacity will be provided at time t).

2) Hydrogen Energy System:

Figure 2 depicts the energy flow among the electrolyzer, the storage tank, fuel cells, and the power grid. Unlike electricity, the hydrogen generated by the electrolyzer can be stored in the tank for later use, such as meeting the vehicle fueling demand and generating power in fuel cells. The operational constraints of the hydrogen energy system can be formulated as:

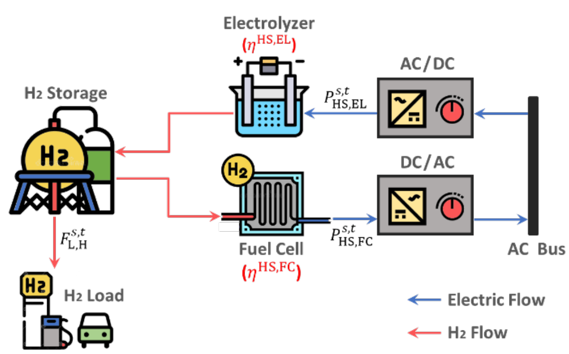

Fig. 2 Illustration of the hydrogen integration process.

$$H_{\mathrm{HS}}^{s,t} = H_{\mathrm{HS}}^{s,t-1} + \left(\eta^{\mathrm{HS,EL}} \cdot P_{\mathrm{HS,EL}}^{s,t} - \frac{1}{\eta^{\mathrm{HS,FC}}} \cdot P_{\mathrm{HS,FC}}^{s,t} - F_{\mathrm{L,H}}^{s,t}\right) \cdot \Delta t, \forall s,t \quad (10)$$

$$0 \le \eta^{\mathrm{HS,EL}} \cdot P_{\mathrm{HS,EL}}^{s,t} \le S_{\mathrm{EL}}, \forall s,t \quad (11)$$

$$0 \le P_{\mathrm{HS,FC}}^{s,t} \le S_{\mathrm{FC}}, \forall s,t \quad (12)$$

$$0 \le H_{\mathrm{HS}}^{s,t} \le S_{\mathrm{tank}}, \forall s,t \quad (13)$$

$$H_{\mathrm{HS}}^{s,0} = H_{\mathrm{HS}}^{s,T} \quad (14)$$

Eq. (10) ensures the hydrogen mass balance, where $H_{\mathrm{HS}}^{s,t}$ denotes the amount of stored hydrogen in the tank at time t. $\eta^{\mathrm{HS,EL}}$ and $\eta^{\mathrm{HS,FC}}$ are the energy conversion efficiency of the electrolyzers and the fuel cells, respectively. Δt denotes the time step. Eq. (11)–(13) restrict the produced hydrogen $\eta^{\mathrm{HS,EL}} \cdot$

$P^{s,t}_{\mathrm{HS,EL}}$, the fuel cell power $P^{s,t}_{\mathrm{HS,FC}}$, and the stored hydrogen $H^{s,t}_{\mathrm{HS}}$ to be within the invested capacity of the related equipment. Eq. (14) enforces that the amount of hydrogen in the tank should be the same at the start and end of each day. The formulation was designed to capture most efficiencies and operating conditions.

3) *PV Module:*

The operational constraints for the PV modules in the integrated system are illustrated as follows:

$$C_{\mathrm{PV,inv}} = c_{\mathrm{PV,inv}} P_{\mathrm{PV,inv}} \tag{15}$$

$$C_{\mathrm{PV,op}} = c_{\mathrm{PV,op}} P_{\mathrm{PV,inv}} \tag{16}$$

$$0 \le P^{s,t}_{\mathrm{PV}} \le P_{\mathrm{PV,inv}}, \forall s, t \tag{17}$$

In Eq. (15) and (16), the PV investment and operation cost depend only on the invested capacity $P_{\mathrm{PV,inv}}$, where $c_{\mathrm{PV,inv}}$ and $c_{\mathrm{PV,op}}$ are the investment and operation cost coefficients. The maximum PV generation is limited to the investment in (17).

4) *Electrical Vehicle:*

For simplicity, we consider only the active power of the EV load, and the operational constraints are as follows:

$$C_{\mathrm{EV,inv}} = c_{\mathrm{EV,inv}} P_{\mathrm{EV,inv}} \tag{18}$$

$$C_{\mathrm{EV,op}} = c_{\mathrm{EV,op}} P_{\mathrm{EV,inv}} \tag{19}$$

$$\gamma_{\mathrm{EV}} P_{\mathrm{EV,inv}} \le P^{s,t}_{\mathrm{EV}} \le P_{\mathrm{EV,inv}} \tag{20}$$

Eq. (18) and (19) calculate the EV investment and the operation costs based on its invested capacity $P_{\mathrm{EV,inv}}$, where $c_{\mathrm{EV,inv}}$ and $c_{\mathrm{EV,op}}$ denote the EV investment and operation cost coefficients. The EV charging load is constrained by (20), where γ_{EV} represents the minimum EV load consumption w.r.t. $P_{\mathrm{EV,inv}}$.

III. Hydrogen Load Simulation

A. *Basic Assumption*

There is a large body of research on EV load modeling [8], but the load demand of hydrogen-fueled vehicles is rarely reported. In this section, we simulate the daily hydrogen load $F^{s,t}_{\mathrm{L,H}}$ based on the data of a hydrogen fueling station in Table I.

Table I Basic Data of The Hydrogen Fueling Station

Asset	Parameter	Value
Hydrogen fueled truck	H_2 tank capacity	33kg
	Fueling time	3–8 minutes
	Driving distance	<250 miles
Hydrogen fueling station	Number of trucks	80–130
	Electrolyzer efficiency	70%
	Fuel cell efficiency	50%
	Electrolyzer capacity	Varies
	Fuel cell capacity	>10MW
	Hydrogen tank capacity	>3,000 kg

Based on the data given, we propose the following assumptions to predict the daily hydrogen load profile:

i. The fueling station works from 9 am to 6 pm daily.

ii. The rate to refuel a hydrogen-fueled truck is constant.

iii. The hydrogen fueling station can serve up to six trucks simultaneously.

iv. Arriving trucks are served in a first-in, first-out order.

v. The interarrival times of trucks $A_1, A_2, \cdots$ are *independent and identically distributed* (IID) random variables that are exponentially distributed with a mean of 5 min.

vi. The fueling times of each truck $T_1, T_2, \cdots$ are IID random variables that are normally distributed with a mean of 5.5 min and a standard deviation of 0.83 min.

According to assumption i, the simulation will begin at 9 am, when there is no truck in the station, and all six dispensers are idle. After A_1 minutes, the first truck will arrive at the station, and it takes T_1 minutes to refuel its tanks. During this process, the first truck contributes $33/T_1$ kg per minute to the hydrogen load (assumption ii). The second truck will arrive at the time $A_1 + A_2$ minutes and will not need to wait if the first truck is served in the station ($T_1 > A_2$) because there are six dispensers; however, if six dispensers are all busy, the following trucks may need to wait in a queue (assumption iii). Moreover, the dispenser will select the truck from the queue based on the first-in, first-out manner (assumption iv). The simulation will be terminated after 9 hours.

From Table I, the number of trucks arriving at the hydrogen fueling station during the 9-hour working day ranges between 80 and 130. Hence, the average interarrival time of trucks is 4.15–6.75 minutes. Any value of the interarrival time, such as 5 minutes, is valid in this range (assumption v). Further, the fueling time of each truck varies from 3 to 8 minutes. We assume the fueling time follows a normal distribution, and the range from 3–8 minutes covers three standard deviations of the mean (99.7% of the fueling time will be within this range). Then assumption vi allows us to easily calculate the mean value and standard deviation.

B. *Simulation Logic*

We first separate the fueling process into two events: the arrival of a truck at the station and the departure of a truck from the station after filling its tank. The logic of these two events is depicted in the flowchart in Fig. 3. At the beginning, the simulation clock is set to 0, and the state variables, such as the number of trucks, will be initialized. The first arrival time is then generated based on assumption *v.* and placed in the initial event list, whereas the departure event is eliminated because no truck is in service. Except for the first event list, we compare the time of the next arrival and departure to determine which event will occur next. Finally, the event with a shorter occurrence time is selected, and the simulation clock is updated to that time.

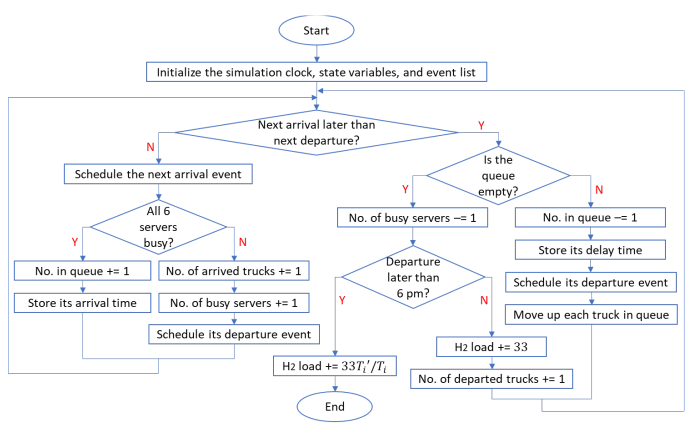

Fig. 3 Flow chart of hydrogen load simulation in the hydrogen fueling station.

If the arrival event is selected, the left part of the flow chart will be implemented first, and the status of the six dispensers in the station needs to be checked. If one or more of them are available, then we will update the state variables and schedule the departure event of this truck based on the assumption vi. On the other hand, if the departure event of the truck is selected, the right part will be implemented. It worth noting that we need to check if the simulation clock exceeds 9 hours for the departure event. The truck cannot be refueled after 6 pm, and its contribution to the hydrogen load will no longer be its total capacity and will be determined by the actual fueling time T_i' ($T_i' < T_i$) instead.

C. Simulation Result

The simulation results of the daily hydrogen load and the number of trucks in the station are illustrated in Fig. 4 (a) and (b), respectively. The profiles of both figures are similar because all fueled trucks have the same tank capacity and constant refueling rate. The peak of the hydrogen load in (a) is 2043.44 kg/h, and the largest number of trucks in service is 5. Hence, all trucks do not need to wait to be fueled in this case.

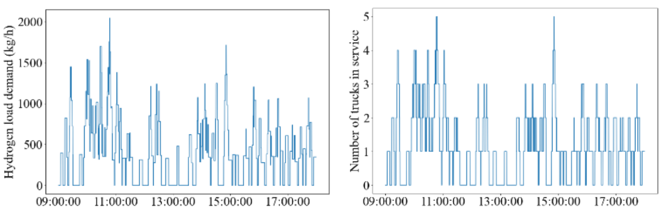

(a) (b)

Fig. 4 Simulation results: (a) the hydrogen load profile on a typical day; (b) the number of hydrogen-fueled trucks in the station.

IV. CASE STUDY

A. Simulation Setup

Uncertainties of load demand $P_{\mathrm{L}}^{s,t}$, PV generation $P_{\mathrm{PV}}^{s,t}$, and market price $\lambda_{\mathrm{mcp}}^{s,t}$ are incorporated into the planning model for the integrated hydrogen energy system. To combine these uncertainties and select the representative scenarios from their one-year historical data [9], we use a K-means clustering method to obtain 21 scenarios representing the winter week, the summer week, and the spring/fall week. The EV load $P_{\mathrm{EV}}^{s,t}$ is calculated from the charging profile of 6 electric school buses and 14 sedan EVs [10]. For the hydrogen load $F_{\mathrm{L,H}}^{s,t}$, the simulation result in Fig. 4 (a) depicts the profile in the winter week. The number of trucks fueled in the station can be a primary determinant of the hydrogen load. Hence, we change the mean of the interarrival time for different truck numbers to simulate 2,000 hydrogen load profiles, and obtain the following profiles for summer and spring/fall weeks by K-means clustering in Fig. 5. Note that the hydrogen load before 9 am and after 6 pm is set as zero.

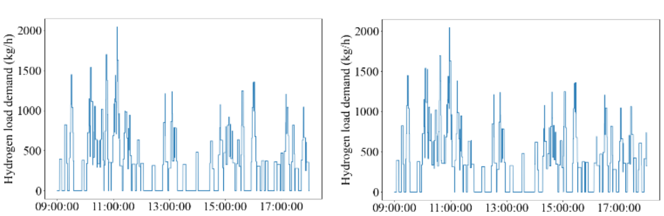

(a) (b)

Fig. 5 Simulation results: (a) hydrogen load profile in summer weeks; (b) hydrogen load profile in spring/fall weeks.

The planning model is implemented with Python and solved with Google OR-Tools [11]. We assume that the planning scheme will last for 10 years, and a summary of the current and future parameters considered planning is shown in Table II.

TABLE II KEY PARAMETERS FOR INTEGRATED SYSTEM PLANNING

Parameter	Current Value	Future Value in 10 Years
$c_{\mathrm{PV,inv}}$	1,640 (\$/kWh) [9]	1,150 (\$/kWh)
c_{tank}	400 (\$/kg) [12]	350 (\$/kg) [12]
c_{EL}	107,800 (\$/kg·h^{-1}) [13]	55,000 (\$/kg·h^{-1}) [14]
c_{FC}	540 (\$/kWh) [14]	200 (\$/kWh) [14]
c_{fixed}	250,000 (\$) [15]	200,000 (\$)
λ_{H}	15 (\$/kg)	8 (\$/kg)
$\eta^{\mathrm{HS,EL}}$	70 (%)	80 (%)
$\eta^{\mathrm{HS,FC}}$	50 (%)	60 (%)
$F_{\mathrm{L,H}}^{s,t}$	Simulation results	One-and-a-half times of simulation results

B. Economic Analysis

In this section, we consider two critical factors in the planning result of the integrated hydrogen energy system. The first factor is whether the demand response and the frequency regulation are considered. In this way, the feasibility of the hydrogen energy system profiting from providing grid services like an energy storage system is further investigated. The second factor is the rapid development of hydrogen refueling technologies, as well as the increasing demand for clean energy, which might help us see the underlying value of investing in the integrated hydrogen energy system in 10 years. Based on these two factors, we design the following three cases:

Case 1: Current-value planning without considering any grid service

Case 2: Current-value planning considering demand response and regulation services

Case 3: Future-value planning considering demand response and regulation services.

TABLE III COMPARISON OF PLANNING RESULTS IN THREE CASES

Case No.	1	2	3
Tank capacity (kg)	3,595.0	3,595.0	5,355.4
Hydrogen production capacity (kg/h)	369.7	369.7	568.0
Fuel cell capacity (kW)	500.0	2,696.2	6,423.3
PV capacity (kW)	500.0	500.0	0.0
EV charger capacity (kW)	160.0	160.0	160.0
Demand response capacity (kW)	0.0	292.3	389.0

The planning results for these three cases are summarized in Table III. Case 2 invests in more fuel-cell capacity than in Case 1 to provide demand response and frequency regulation. In comparison to Case 2, the tank, electrolyzer, and fuel cell capacity in Case 3 are much more prominent due to the increasing hydrogen load in the future. There is no PV investment in this case because the fuel cell capacity is sufficient to support the load. Moreover, the demand response capacity of Case 3 is the largest, thanks to the highest fuel cell capacity.

Table IV displays all terms of the objective function. Note that the listed planning expenses and the revenue are discounted into their annuity payment and annual income. The first four terms in Table IV form the investment cost of the hydrogen energy system as shown in Eq. (3). Among them, most of the investment cost is assigned to the electrolyzers, indicating the significance of reducing their cost in the future. The operation cost in Eq. (4) is further divided into two parts in this table: the energy procurement bill and the device operating cost.

We first compare the results of Case 1 and Case 2. It can be observed that less electricity is purchased while a higher grid-side income is obtained in Case 2 due to the energy arbitrage from grid services. Further, the penalty to not provide adequate grid services in Case 2 is much lower than in Case 1.

TABLE IV DISCOUNTED PLANNING EXPENSES AND REVENUE IN THREE CASES

Case No.	1	2	3
Tank capital cost (k$/yr)	177.36	177.36	231.19
Electrolyzer capital cost (k$/yr)	4,915.40	4,915.40	3,852.91
Fuel cell capital cost (k$/yr)	33.30	179.57	158.45
Annual fixed cost (k$/yr)	30.83	30.83	24.67
PV capital cost (k$/yr)	101.14	101.14	0
EV capital cost (k$/yr)	3.95	3.95	3.95
Energy procurement bill (k$/yr)	501.29	184.42	4.00
Device operating cost (k$/yr)	6,399.47	6,577.36	5,194.47
Grid-side income (k$/yr)	59.08	229.85	346.53
Hydrogen revenue (k$/yr)	18,516.11	18,516.11	14,812.89
Annual penalty (k$/yr)	1,275.36	19.43	32.24
Hydrogen-system income (k$/yr)	5,137.08	6,556.49	5,657.54

Based on the predicted future parameters in Table II, the hydrogen load increases, and its compensation price decreases in 10 years. Hence, the integrated system in Case 3 is expected to have the highest capacity. The fuel cells in the system can act as the battery to shift the peak load and provide additional grid services, which is reflected by the lowest energy procurement bill and the highest grid-side income in Case 3; however, the hydrogen price decreases more rapidly than the increase of the hydrogen load, resulting in a lower hydrogen income in Case 3 than Case 2. Because the hydrogen income has the most significant impact on the objective value, the final revenue earned in Case 3 is less than that in Case 2, demonstrating the current economy of investing in the integrated system.

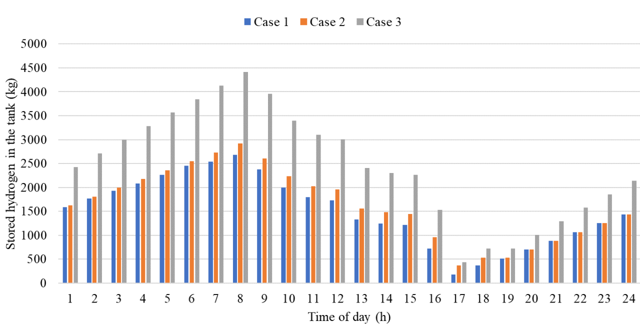

Fig. 6 Comparison of the daily stored hydrogen in three cases.

The profiles of the stored hydrogen in a typical winter scenario of three cases are illustrated in Fig. 6. Due to a much higher hydrogen load in the future, Case 3 has the highest amount of hydrogen stored. The results of Case 1 and Case 2 make very little difference.

V. CONCLUSIONS

This formulation demonstrated performance-based value stacking of different services under current and future investment scenarios. We considered the revenue from providing grid services and selling hydrogen fuel in an integrated hydrogen energy system. The optimal capacities of the hydrogen storage tank, electrolyzers, fuel cells, PV, and EV charging modules were obtained in the planning result. From the case study, we demonstrated that the profitability of the planning model will increase by 27.63% with consideration of providing grid services when comparing Case 1 with Case 2. The investment in hydrogen storage and electrolyzers was similar when i) supporting the base operations of the integrated system only (Case 1) and ii) participating in grid service markets (Case 2). However, the investment in fuel-cell capacity increased for Case 2 – primarily due to the value stacking of the hydrogen systems through multiple services. Both cases assume current investment and price trends. The hydrogen system dispatch helped Case 2 increase the overall revenue via additional services and reduced costs from demand and load management. Assuming growth in hydrogen demand to H2@SCALE markets, combined with cheaper hydrogen selling prices and lower capital costs (Case 3) – our analysis indicates an increased investment in the hydrogen storage capacity. At the same time, the profitability of Case 3 decreases by 15.89% when compared with Case 2 – due to lower revenue from selling hydrogen.

REFERENCES

[1] J. P. Barton, and D. G. Infield, "Energy storage and its use with intermittent renewable energy," *IEEE Transactions on Energy Conversion*, vol. 19, no. 2, pp. 441–448, May. 2014.

[2] E. Rivard, M. Trudeau, and K. Zaghib, "Hydrogen storage for mobility: a review," *Materials*, vol. 12, no. 12, p. 1973, Jun. 2019.

[3] P. Colbertaldo, S. B. Agustin, S. Campanari, *et al.*, "Impact of hydrogen energy storage on California electric power system: Towards 100% renewable electricity," *International Journal of Hydrogen Energy*, vol. 44, no. 19, pp. 9558–9576, Apr. 2019.

[4] F. Khalid, I. Dincer, and M. A. Rosen, "Analysis and assessment of an integrated hydrogen energy system," *International Journal of Hydrogen Energy*, vol. 41, no. 19, pp. 7960–7967, May. 2016.

[5] A. H. Schrotenboer, A. A. Veenstra, M. A. uit het Broek, *et al.*, "A green hydrogen energy system: optimal control strategies for integrated hydrogen storage and power generation with wind energy," *Renewable and Sustainable Energy Reviews*, vol. 168, p. 112744, Oct. 2022.

[6] J. Zhang, C. Li, G. Chen, *et al.*, "Planning of hydrogen refueling stations in urban setting while considering hydrogen redistribution," *IEEE Transactions on Industry Applications*, vol. 58, no. 2, pp. 2898–2908, Oct. 2021.

[7] J. Morel, S. Y. Obara, K. Sato, *et al.*, "Contribution of a hydrogen storage-transportation system to the frequency regulation of a microgrid," *International Conference on Renewable Energy Research and Applications (ICRERA)*, pp. 510–514, Nov. 2015.

[8] J. Yan, J. Zhang, Y. Liu, *et al.*, "EV charging load simulation and forecasting considering traffic jam and weather to support the integration of renewables and EVs," *Renewable Energy*, vol. 159, pp. 623–641, Oct. 2020.

[9] W. Liu, Y. Yao, R. Jain, *et al.*, "Commercial building planning and retrofitting strategy for grid services," *IEEE/PES Transmission and Distribution Conference and Exposition (T&D)*, pp. 1–5, April. 2022.

[10] R. Jain, S. Veda, W. Becker, *et al.*, "Application of site controllers for electrification of commercial fleet vehicles," *IEEE/PES Transmission and Distribution Conference and Exposition (T&D)*, pp. 1–5, Oct. 2020.

[11] Google OR-Tools. [Online]. Available: https://developers.google.com/optimization

[12] B. D. James, C. Houchins, J. M. Huya-Kouadio, *et al.*, "Hydrogen storage system cost analysis," Strategic Analysis Inc., Arlington, VA, USA, *Tech. Rep. DOE-SA-0005253 7037787114*, 2016.

[13] P. Graham, J. Hayward, J. Foster, *et al.*, "GenCost 2021-22: Final report," CSIRO, Australia, Jul. 2022.

[14] J. Hinkley, J. Hayward, R. McNaughton, *et al.*, "Cost assessment of hydrogen production from PV and electrolysis," Report to ARENA as part of Solar Fuels Roadmap, Project A-3018, pp. 1–4, Mar. 2016.

[15] K. Reddi, A. Elgowainy, N. Rustagi, et al., "Impact of hydrogen refueling configurations and market parameters on the refueling cost of hydrogen," *International Journal of Hydrogen Energy*, vol. 42, no. 34, pp. 21855–21865, Aug. 2017.